

Original Article

The role of ezrin-associated protein network in human sperm capacitation

Lei Wang¹, Wen Chen¹, Chun Zhao¹, Ran Huo¹, Xue-Jiang Guo¹, Min Lin¹, Xiao-Yan Huang¹, Yun-Dong Mao^{1,2}, Zuo-Min Zhou¹, Jia-Hao Sha¹

¹Laboratory of Reproductive Medicine, Department of Histology and Embryology, Nanjing Medical University, Nanjing 210029, China

²Department of Reproductive Medicine, the First Affiliated Hospital of Nanjing Medical University, Nanjing 210029, China

Abstract

Membrane modifications in sperm cells represent a key step in sperm capacitation; however, the molecular basis of these modifications is not fully understood. Ezrin is the best-studied member of the ezrin/radixin/merlin family. As a cross-linker between the cortical cytoskeleton and plasma membrane proteins, ezrin contributes to remodeling of the membrane surface structure. Furthermore, activated ezrin and the Rho dissociation inhibitor, RhoGDI, promote the formation of cortical cytoskeleton-polymerized actin through Rho activation. Thus, ezrin, actin, RhoGDI, Rho and plasma membrane proteins form a complicated network *in vivo*, which contributes to the assembly of the structure of the membrane surface. Previously, we showed that ezrin and RhoGDI1 are expressed in human testes. Thus, we sought to determine whether the ezrin–RhoGDI1–actin–membrane protein network has a role in human sperm capacitation. Our results by Western blot indicate that ezrin is activated by phosphorylation of the threonine567 residue during capacitation. Co-immunoprecipitation studies revealed that, during sperm capacitation, the interaction between ezrin and RhoGDI1 increases, and phosphostaining of two dimensional electrophoresis gels showed that RhoGDI1 is phosphorylated, suggesting that RhoGDI1 dissociates from RhoA and leads to actin polymerization on the sperm head. We speculate that activated ezrin interacts with polymerized actin and the glycosylated membrane protein cd44 after capacitation. Blocking sperm capacitation using ezrin- or actin-specific monoclonal antibodies decreases their acrosome reaction (AR) rate, but has no effect on the AR alone. Taken together, our results show that a network consisting of ezrin, RhoGDI1, RhoA, F-actin and membrane proteins functions to influence the modifications that occur on the membrane of the sperm head during human sperm capacitation.

Asian Journal of Andrology (2010) 12: 667–676. doi: 10.1038/aja.2010.79; published online 16 August 2010.

Keywords: ezrin, membrane, sperm capacitation

Correspondence to: Dr Yun-Dong Mao and Dr Zuo-Min Zhou, Laboratory of Reproductive Medicine, Department of Histology and Embryology, Nanjing Medical University, 140 Hanzhong Road, Nanjing 210029, China.

Fax: +86-25-8686-2908

E-mail: drmaoyd@yahoo.com.cn and zhouzm@njm.edu.cn

Received: 29 March 2010 Revised: 28 April 2010

Accepted: 11 June 2010 Published online: 16 August 2010

1 Introduction

Highly differentiated and polarized human spermatozoa need to fulfil various requirements before fertilization. The preparative events that render the spermatozoa competent for fertilization are collectively known as capacitation. Capacitation is a process that takes



place *in vivo* after the spermatozoa have been inside the female genital tract for a period of time or *in vitro* under certain culture conditions. During capacitation, modifications in the distribution of proteins on the sperm surface, alterations in the characteristics of the plasma membrane, changes in enzyme activities and changes in the expression of intracellular constituents render these cells responsive to stimuli that induce the acrosome reaction (AR) before fertilization. The major changes occur at the sperm plasma membrane, which confers them with the ability to be fusogenic and responsive to glycoproteins of the zona pellucida [1–4]. In the past 50 years since Austin [5] and Chang [6] first defined capacitation, many groups have focused their research on the modifications that the sperm plasma membrane undergoes during capacitation, and their efforts have generated some progress in this area [1, 2, 7–10]. Most studies have shown that increased membrane fluidity is a key modification that occurs at the sperm plasma membrane, a change that may be regulated by cholesterol efflux and is accompanied by changes in the dynamics of lipid rafts and relocalization of membrane proteins. However, the exact mechanism of how these modifications occur is not completely understood.

The ezrin/radixin/merlin (ERM) family consists of three closely related proteins: ezrin, radixin and moesin. Ezrin is the best-studied member of the ERM family, which was first isolated as a component of microvilli from chicken intestinal brush borders [11], and is reported to function as a cross-linker between the cortical cytoskeleton and membrane proteins. Ezrin has been shown to localize beneath the plasma membrane in regions containing densely packed actin filaments and in cellular structures, such as microvilli, ruffling membranes and cell–cell and cell–substrate adhesion sites [12–14]. Based on its localization and protein-binding activity, ezrin is suggested to be involved in the regulation of a variety of cellular processes. Ezrin exists in two functionally different states. In its inactive state, the C-terminal domain is associated with the N-terminal domain, causing ezrin to acquire a ‘closed’ conformation. On activation of ezrin by the phosphorylation of threonine₅₆₇ (Thr₅₆₇) in the C-terminal domain, the interaction between the N- and C-terminal domains is disrupted, exposing a binding site that is critical for membrane–cytoskeleton interactions [15, 16]. Interestingly, ezrin has also been shown to regulate the polymerization of actin. Ezrin can interact directly with RhoGDI and dissociate it from Rho-GTPases, allowing

the GTPases to become loaded with GTP and become subsequently activated. Taken together, these findings indicate an important role for ezrin in the activation of the Rho family members and in the consequent promotion of actin polymerization [17–19].

Recently, Brener *et al.* [20], Breitbart *et al.* [21–23] and Liu *et al.* [24–26] have focused their studies on the role of the cytoskeletal network on sperm capacitation, and they showed that during capacitation, F-actin is generated and has a role in the AR and fertilization [20–26], which provides a strong basis for our work. We previously showed that ezrin and RhoGDI1 are expressed in human testes [27]. Because previous findings in somatic cells suggest that the expression of these two proteins is associated with remodeling of the plasma membrane [13, 14], we speculated that a protein network composed of ezrin, RhoGDI1 and their associated proteins may exist in human sperm and possibly have a role in capacitation. Therefore, the aim of the present study was to determine whether such a molecular protein network exists in human sperm and, if so, to examine its role in capacitation. We reasoned that this work would also advance our understanding of the process of capacitation.

2 Materials and methods

2.1 Sperm preparation

Before initiating the study, consent was obtained from all participants. The semen samples were obtained by masturbation after at least 3 days of abstinence from 10 healthy male volunteers of proven fertility and with normal semen quality, as assessed by World Health Organization criteria (1999) [28]. The samples were ejaculated into sterile containers and allowed to liquefy for at least 30 min before being processed by centrifugation in a 60% Percoll gradient (GE Healthcare, Waukesha, WI, USA) to remove round cells.

2.2 Sperm capacitation

After centrifugation, sperm were washed twice with BWW medium (114.00 mmol L⁻¹ NaCl, 4.78 mmol L⁻¹ KCl, 1.71 mmol L⁻¹ CaCl₂, 1.19 mmol L⁻¹ MgSO₄, 1.19 mmol L⁻¹ KH₂PO₄, 21.58 mmol L⁻¹ sodium lactate, 5.56 mmol L⁻¹ glucose, 10.00 mmol L⁻¹ HEPES (4-[2-hydroxyethyl]-1-piperazineethanesulfonic acid), 25.07 mmol L⁻¹ NaHCO₃ and 10% fetal bovine serum (pH 7.6) and resuspended in BWW at a final density of 50 × 10⁶ cells per mL. The samples were incubated in this capacitation medium for 2.5 and 5 h at 37°C in an atmosphere of 5% CO₂.

2.3 Western blot

The sperm samples were washed twice with PBS, lysed in lysis buffer (7 mol L⁻¹ urea, 2 mol L⁻¹ thiourea, 4% [w/v] CHAPS, 2% [w/v] dithiothreitol [DTT], 1 mmol L⁻¹ NaF and 1 mmol L⁻¹ Na₂VO₃·12H₂O) supplemented with 1% (v/v) protease inhibitor cocktail (Pierce, Rockford, IL, USA) and homogenized at 11 000 r.p.m. for 5 min on ice. The lysates were then incubated for 1 h at 4°C. After centrifugation at 12 000 × g at 4°C for 30 min, the supernatants were collected and stored at -70°C until use.

The protein concentration of the lysates was determined using the Bradford assay. The proteins were then separated on 12% SDS-polyacrylamide gels and transferred onto nitrocellulose membranes under semi-dry conditions using the Hoefer SemiPhor system (GE Healthcare). The membranes were blocked in 5% non-fat milk in Tris-buffered saline (TBS; pH 7.4) for 1 h before being incubated with ezrin monoclonal antibody (mAb; 1:500; Zymed Laboratories Inc., South San Francisco, CA, USA), rabbit RhoGDI1 antibody (1:1 000; Santa Cruz Biotechnology, Santa Cruz, CA, USA), rabbit cd44 antibody (1:500; Santa Cruz Biotechnology), rabbit tubulin antibody (1:2 000; Abcam, Cambridge, MA, USA) or rabbit anti-phosphoezrin (Thr₅₆₇)/radixin (Thr₅₆₄)/moesin (Thr₅₅₈) antibody (1:500; Cell Signaling Technology, Danvers, MA, USA) diluted in blocking solution at 4°C overnight. The membranes were then washed three times in TBS and incubated with peroxidase-conjugated goat anti-mouse or goat anti-rabbit immunoglobulin G (IgG) antibody (1:1 000; Beijing ZhongShan Biotechnology Co., Beijing, China) for 1 h at 37°C. After washing, an enhanced chemiluminescence reaction kit (GE Healthcare) was used to detect peroxidase activity, and images of the developed membranes were captured using the FluorChem 5500 system (Alpha Innotech, San Leandro, CA, USA).

2.4 Co-immunoprecipitation (Co-IP)

Spermatozoa from at least three healthy volunteers were lysed, as described above, using RIPA buffer (1% [v/v] NP-40, 0.1% [w/v] SDS, 0.5% [w/v] sodium deoxycholate, 0.05 mol L⁻¹ Tris, 0.15 mol L⁻¹ NaCl, 1 mmol L⁻¹ NaF and 1 mmol L⁻¹ Na₂VO₃·12H₂O) supplemented with 1% (v/v) protease inhibitor cocktail (Pierce) instead of lysis buffer. The lysates were mixed, precleared with 50 µL of protein A agarose slurry (Invitrogen, Carlsbad, CA, USA) and rotated for 30 min at 4°C. For immunoprecipitation, the precleared samples

were incubated with antibodies overnight at 4°C. After the addition of 100 µL of protein A agarose slurry, the mixtures were rotated for 2 h at 4°C. The samples were then washed three times with RIPA buffer by centrifugation at 14 000 × g for 10 s at 4°C and boiled in 50 µL of SDS buffer for 5 min. The samples were then separated on 12% SDS-polyacrylamide gel electrophoresis gels and subjected to western blot analysis, as described above.

2.5 Immunofluorescence

For immunofluorescence analysis, the spermatozoa samples were spread onto microscope slides and allowed to air-dry. The samples were then fixed with 4% paraformaldehyde in phosphate-buffered saline (PBS) for 40 min and permeabilized with 0.2% Triton X-100 in PBS for 20 min at 37°C. After three 5-min washes with PBS, the slides were blocked with goat serum (Beijing ZhongShan Biotechnology Co.) diluted in PBS for 1 h and then incubated with ezrin mAb (1:250), rabbit RhoGDI1 antibody (1:500) or rabbit cd44 antibody (1:100) overnight. After incubation with fluorescein isothiocyanate (FITC)- or TRITC (Tetramethylrhodamine-5-[and 6]-isothiocyanate)-conjugated goat anti-mouse or anti-rabbit IgG (1:100; Beijing ZhongShan Biotechnology Co.) for 1 h, the slides were washed in PBS and covered with a coverslip. The slides were viewed using an Axioskop 2 Plus microscope (Carl Zeiss, Oberkochen, Germany) with a × 100 oil objective, and the images were captured with a CCD camera (Carl Zeiss) using AxioVersion 4.5 software (Carl Zeiss). The negative controls were incubated with an isotype mAb or normal rabbit serum (Santa Cruz Biotechnology) instead of the primary antibody.

2.6 Fluorescence staining of F-actin

The sperm samples were spread onto microscope slides, fixed and permeabilized, as described above. The slides were incubated at room temperature (RT) with 1% bovine serum albumin in PBS for 2 h and then with Texas Red-conjugated phalloidin (Invitrogen) for 20 min. Actin polymerization was analyzed using a Zeiss fluorescent microscope, as described above.

2.7 Two-dimensional electrophoresis (2-DE), protein spot detection, in-gel tryptic digestion, matrix-assisted laser desorption/ionization time-of-flight mass spectrometer (MALDI-TOF MS), database searching and detection of phosphorylated proteins

Protein (80 µg) from uncapacitated or capacitated

sperm from three fertile donors was prepared for 2-DE, which was performed as described previously [29]. The proteins on the gels were visualized by silver or phosphorylation staining with the Pro-Q Diamond phosphoprotein gel stain kit (Invitrogen) following the manufacturer's instructions.

The silver-stained gels were scanned using the Atrix Scan 1010 plus (Microtek, Taiwan, China), and the resulting images were analyzed using ImageMaster 2D Platinum software (GE Healthcare) for protein spot detection, quantification and comparative and statistical analyses. The spot volumes of the proteins from each experimental group were pooled to calculate the mean \pm SD. relative volume, and an independent *t*-test was performed to determine the significance of the differences between the two groups. $P < 0.05$ were considered statistically significant.

The protein spots obtained by 2-DE were then excised, dehydrated in acetonitrile and dried at room temperature. The proteins were reduced with 10 mmol L⁻¹ DTT/25 mmol L⁻¹ NH₄HCO₃ at 56°C for 1 h and alkylated with 55 mmol L⁻¹ iodoacetamide/25 mmol L⁻¹ NH₄HCO₃ in the dark and at room temperature for 45 min *in situ*. The gel fragments were thoroughly washed with 25 mmol L⁻¹ NH₄HCO₃, 50% acetonitrile and 100% acetonitrile and dried in a Speedvac. The dried fragments were rehydrated in 2–3 μ L of a 10-ng μ L⁻¹ solution of trypsin (Promega, Madison, WI, USA) in 25 mmol L⁻¹ NH₄HCO₃ at 4°C for 30 min. The excess liquid was discarded, and the gel plugs were incubated at 37°C for 12 h to allow for digestion of the gel. Trifluoroacetic acid (TFA) was added to a final concentration of 0.1% to stop the digestion.

The digests were immediately spotted onto 600- μ m AnchorChips (Bruker Daltonics, Bremen, Germany). Spotting was achieved by pipetting 1 μ L of each digest, in duplicate, onto the MALDI target plate and then adding 0.05 μ L of 2 g L⁻¹ α -HCCA in 0.1% TFA/33% acetonitrile supplemented with 2 mmol L⁻¹ ammonium phosphate. The Bruker Peptide Calibration Mixture was also spotted onto the plate for external calibration. All samples were allowed to air-dry at room temperature, and 0.1% TFA was used for on-target washing. MALDI-TOF MS was carried out using a time-of-flight Ultraflex II mass spectrometer (Bruker Daltonics). Mass maps for the peptides were acquired in the positive reflection mode, averaging 800 laser shots per MALDI-TOF spectrum (at a resolution of 15 000–20 000). The Bruker Peptide Calibration Mixture was used to calibrate the spectrum to a mass

tolerance within 0.1 Da.

For the database search, each acquired mass spectrum (*m/z*, range 700–4 000) was processed using FlexAnalysis v2.4 software (Bruker Daltonics) using the following parameters: peak detection algorithm: Sort Neaten Assign and Place; S/N threshold: 3; quality factor threshold: 50. The trypsin autodigestion ion peaks (842.51 Da and 2 211.10 Da) were used as internal standards to validate the external calibration procedure. The matrix and/or autoproteolytic trypsin fragments and any known ion contaminants (keratins) were excluded from the analysis. The peptide masses obtained were used to search the Swiss-Prot database (<http://www.matrixscience.com/>) (241 242 sequences, 88 541 632 residues, for Human 15 057 sequences) using Mascot (v2.1.03; Matrix Science, Boston, MA, USA) in the automated mode. The following search parameters were used: significant protein MOWSE (molecular weight search) score: $P < 0.05$; minimum mass accuracy: 100 p.p.m.; trypsin as the enzyme; one missed cleavage site allowed; cysteine carbamidomethylation; acrylamide-modified cysteine; methionine oxidation; similarity of isoelectric point and relative molecular mass specified; and minimum sequence coverage: 15%.

For the detection of phosphorylated proteins, the gels were fixed in 50% methanol/10% acetic acid overnight, washed three times with deionized water, incubated in Pro-Q Diamond phosphoprotein gel stain for 90 min and destained by washing three times with 20% ACN in 50 mmol L⁻¹ sodium acetate (pH 4.0) and two times with deionized water. Images of the gels were acquired using the Typhoon Variable Model Imagels 9400 system (GE Healthcare) at an excitation wavelength of 532 nm and a 580-nm band pass emission filter.

2.8 Deglycosylation of sperm proteins

The sperm proteins were deglycosylated using PNGase F (Sigma-Aldrich, St. Louis, MO, USA) according to the manufacturer's instructions with slight modifications. Briefly, proteins from the capacitated sperm were extracted, as described above, diluted in 20 mmol L⁻¹ NH₄HCO₃ (pH 7.5) and denatured by boiling at 100°C for 10 min in denaturing solution (10% SDS and 1 mol L⁻¹ DTT). After the addition of 6 μ L of PNGase F enzyme solution (500 000 U L⁻¹), the mixture was incubated at 37°C overnight. For the controls, PNGase F was omitted. The deglycosylated proteins were then subjected to Western blot analysis using a rabbit cd44 antibody.

2.9 Assessment of acrosome status

The acrosome status of the sperm was determined using FITC-labelled *Pisum sativum agglutinin* (PSA; Sigma-Aldrich), as described previously [24]. Briefly, sperm smears were air-dried, fixed in 95% ethanol for 30 min and stained with 25 mg L⁻¹ PSA in PBS for 2 h at RT. The slides were then washed with distilled water and mounted, and the sperm were counted using a fluorescence microscope.

2.10 Effects of ezrin and actin depletion on capacitation and the A23187-induced AR

Inhibition of capacitation using various concentrations of anti-ezrin (Sigma-Aldrich) and anti-actin (MP Biomedicals, Solon, OH, USA) mAbs was performed as follows. Motile sperm cultured in BWW were mixed with 1:10 to 1:80 dilutions of anti-ezrin, anti-actin or control mAb (1:10) for 5 h at 37°C in an atmosphere of 5% CO₂, followed by the addition of A23187 (Sigma-Aldrich) to induce the AR. The inhibition of the A23187-induced AR using various concentrations of anti-ezrin or anti-actin mAb was performed, as just described, with the exception that the mAbs were added to the medium immediately before the addition of A23187. Each experiment was repeated at least three times with sperm samples from at least three different subjects.

2.11 Statistical analysis

To assess the effects of mAb-mediated depletion of ezrin or actin on sperm capacitation and the AR, we calculated the percentage of sperm treated with the appropriate mAb or with BWW that underwent the AR. The data are expressed as mean ± SD % AR. One-way analysis of variance (ANOVA) was used for statistical analysis. All ratios were transformed using the arcsine square root before performing ANOVA by SPSS version 10.0 (SPSS Inc., Chicago, IL, USA), and the least significant difference *post hoc* test was used to examine any significant differences between groups with equal variance. $P < 0.05$ were considered statistically significant.

3 Results

3.1. Expression of ezrin and RhoGDI1 in human sperm

To determine whether ezrin and RhoGDI1 were expressed in human sperm, we performed Western blot analysis of human sperm proteins and identified bands of ~82 and ~23 kDa, consistent with the predicted molecu-

lar weights of ezrin and RhoGDI1, respectively (Figure 1A). Immunofluorescence studies showed that ezrin and RhoGDI1 are expressed in the acrosome region of the sperm head and in the tail (Figure 1B). Dual-immunofluorescence staining showed colocalization of ezrin and RhoGDI1 in the acrosome region (Figure 1C), suggesting that these proteins may interact in the sperm head.

3.2. Roles of ezrin and RhoGDI1 in actin polymerization during capacitation

Because ezrin is activated by phosphorylation of the Thr₅₆₇ residue, we performed a Western blot with the sperm samples using an antibody against rabbit anti-phospho-ezrin (Thr₅₆₇)/radixin (Thr₅₆₄)/moesin (Thr₅₅₈). Our results show that phosphorylation of ezrin on Thr₅₆₇ increases during capacitation (Figure 2A). Using 2-DE, we identified two spots for RhoGDI1 from the sperm proteins before and after capacitation (Figure 2B and

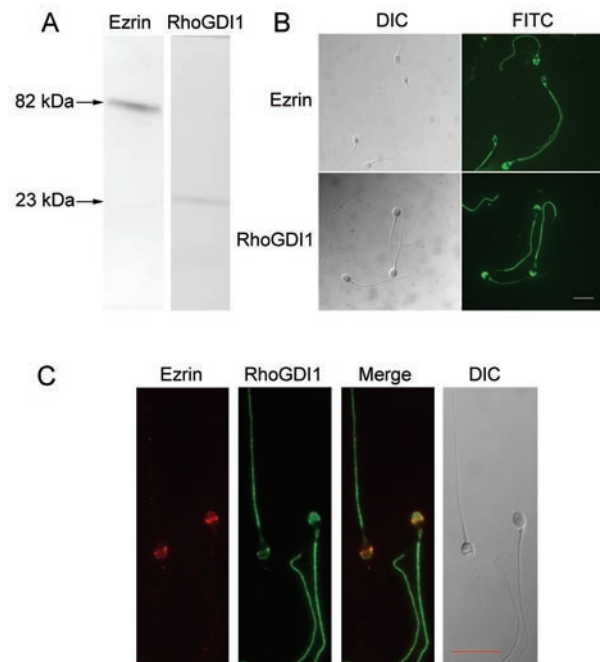


Figure 1. Expression of ezrin and RhoGDI1 in human sperm. (A): Western blot of human sperm lysates probed with ezrin- and RhoGDI1-specific antibodies showing single bands of ~82 and ~23 kDa, respectively. (B): Immunofluorescence labeling of ezrin and RhoGDI1 in human sperm showing that both proteins are expressed in the acrosome and flagellum of human sperm. (C): Dual-immunofluorescence staining of ezrin (red) and RhoGDI1 (green) in human sperm showing that the two proteins colocalize in the sperm acrosome and tail. DIC, dynein intermediate chain; FITC, fluorescein isothiocyanate. Bars = 10 μ m.

Table 1). A comparison of the relative volumes of the two spots indicated an increase in spot 1 and a decrease in spot 2 after capacitation (Figure 2B), which may be indicative of phosphorylation. Furthermore, our hypothesis that RhoGDI1 is phosphorylated during capacitation was supported by phosphorylation staining of the 2-D gels (Figure 2B). Co-IP assays further confirmed that ezrin and RhoGDI1 interact during capacitation, which leads to the release of RhoA from RhoGDI1 after capacitation (Figure 2C). Using Texas Red phalloidin staining, we also observed the formation of F-actin during capacitation (Figure 2D).

3.3 Ezrin interacts with polymerized actin and the membrane protein cd44 during capacitation

As in somatic cells, our findings show that ezrin can interact with actin during capacitation (Figure 3A). Our results are consistent with those published by Bains *et al.* [30] showing that cd44 is expressed in human sperm (Figure 3B) and is localized to the acrosome and tail (Figure 3C). By Western blot, two additional bands above the predicted size were observed for the capacitated sperm proteins, whereas uncapacitated sperm proteins only yielded one predicted band (Figure 3B). Because previous studies showed that cd44 has multiple glycosylation sites [31], we used PNGase F to deglycosylate the proteins extracted from the capacitated human sperm, and the results confirmed that cd44 was indeed glycosylated during capacitation (Figure 3D). Subsequently, we performed a Co-IP assay for ezrin and cd44, and we found that ezrin interacts with the glycosylated and native forms of cd44 after capacitation (Figure 3E).

3.4 Effects of ezrin and actin depletion on capacitation and the A23187-induced AR

When anti-ezrin and anti-actin mAbs were added to the culture medium before capacitation, the A23187-induced AR decreased ($P < 0.05$ and $P < 0.01$, respectively, Figure 4A). However, when the mAbs were added after capacitation and immediately before the addition of A23187, there were no significant differences ($P > 0.05$) in the percentage of AR between the mAb-treated groups and the controls (Figure 4B). These findings suggest that the depletion of ezrin or actin through mAb treatment only inhibits capacitation but has no effect on the A23187-induced AR.

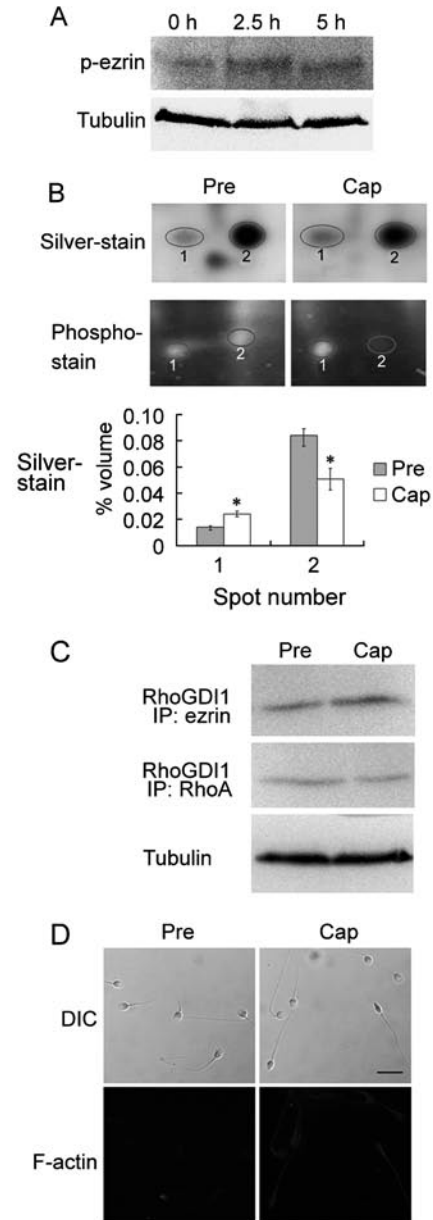


Figure 2. Roles of ezrin and RhoGDI1 in actin polymerization during capacitation. (A): Western blot analysis of human sperm lysates extracted before and after capacitation for 2.5 or 5 h. The blots were probed with rabbit anti-phospho-ezrin (Thr₅₆₇)/radixin (Thr₅₆₄)/moesin (Thr₅₅₈) antibody (p-ezrin). (B): Differential expression of RhoGDI1 before and after capacitation, as analyzed by two-dimensional electrophoresis analysis. The gels were stained with the silver or Pro-Q Diamond phosphoprotein gel stain kit. The graph (bottom) depicts the quantification of the silver-stained spots. * $P < 0.01$, compared with before capacitation. (C): Co-immunoprecipitation assay with ezrin and RhoA antibodies for pull down and RhoGDI1 antibody for detection. (D): Comparison of F-actin expression in human sperm before and after capacitation using Texas Red-conjugated phalloidin staining. Cap, capacitation; DIC, dynein intermediate chain; Pre, before capacitation. Bar = 10 μ m.

Table 1. RhoGDI1 identification by mass spectrometry and database searches.

| Spot ID | Accession number | Protein name | Score | Expect | Matched/searched | Coverage |
|---------|------------------|--|-------|----------------------|------------------|----------|
| 1 | P52565 | Rho GDP-dissociation inhibitor 1 (RhoGDI1) | 120 | 1.5×10^{-8} | 12/31 | 35% |
| 2 | P52565 | Rho GDP-dissociation inhibitor 1 (RhoGDI1) | 122 | 9.5×10^{-9} | 13/51 | 35% |

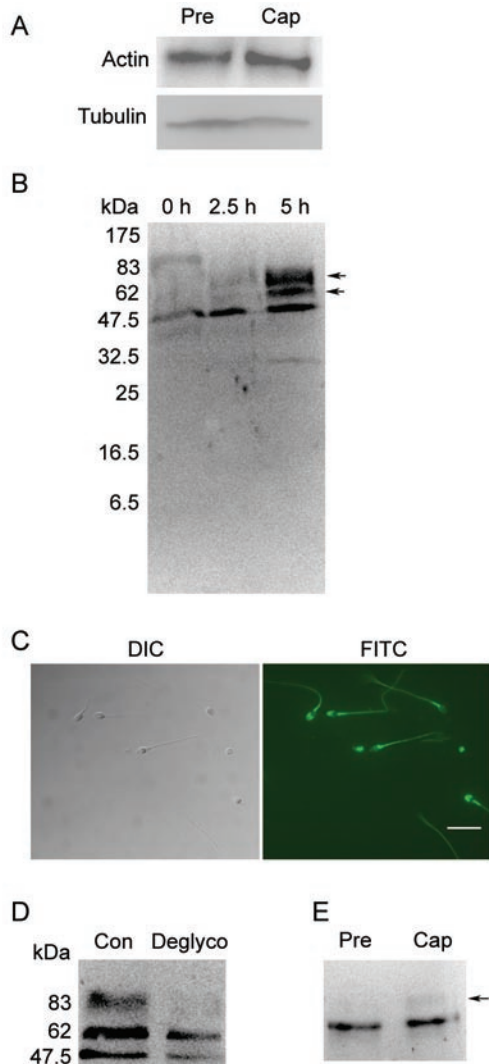


Figure 3. Ezrin interacts with polymerized actin and the membrane protein cd44 during capacitation. (A): Co-IP assay using an ezrin-specific mAb for pull down and an actin-specific antibody for detection. (B): Western blot analysis of cd44 expression in human sperm before (0 h), during (2.5 h) and after (5 h) capacitation. The blot shows the presence of two protein bands after capacitation (arrow). (C): Immunofluorescence staining of cd44 in human sperm. Bar = 10 μ m. (D): Western blot analysis of cd44 expression in capacitated sperm extracts pre-treated with (Deglyco) or without (Con) PNGase F. (E): Co-immunoprecipitation assay using an ezrin-specific mAb for pull down and a cd44-specific antibody for detection. The arrow depicts the band that pertains to glycosylated cd44. Cap, capacitation; DIC, dynein intermediate chain; FITC, fluorescein isothiocyanate; Pre, before capacitation.

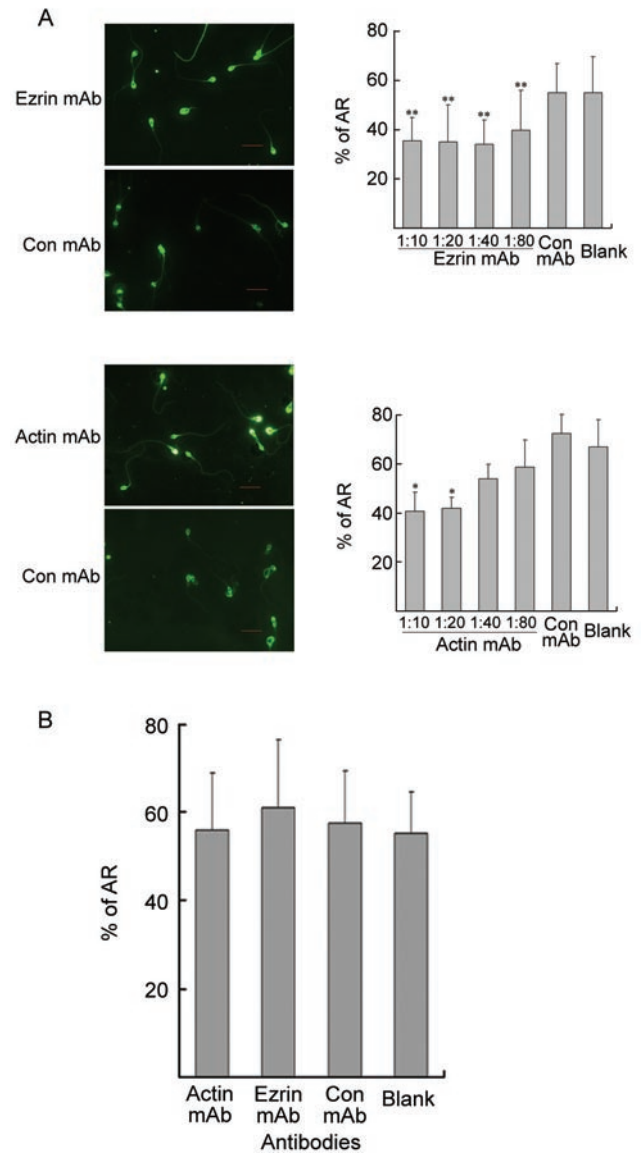


Figure 4. Assessment of the acrosome reaction (AR). (A): The sperm were incubated in BWW alone (blank) or in the presence of different concentrations of ezrin, actin or control (Con) mAb during capacitation for 5 h before induction of the AR using A23187. Bars = 10 μ m. The results were quantified and graphed, as shown on the right (mean \pm SD % AR). * $P < 0.01$, ** $P < 0.05$, compared with the blank. (B): During the A23187-induced AR, capacitated sperm were incubated in BWW alone (blank) or in the presence of ezrin, actin (1:10) or control (Con) mAb (mean \pm SD % AR).

4 Discussion

Recently, some groups have focused their research on the role of the cytoskeletal network on sperm capacitation [20–26]. Breitbart *et al.* [21] showed that actin polymerizes during sperm capacitation and that inhibition of F-actin formation by cytochalasin D blocks capacitation. Further studies using an *in vitro* culture assay showed that actin moves to the surface of the sperm head during capacitation, a process which may have a role in membrane modification during this process [25]. Although these reports studied the role of F-actin during sperm capacitation, a number of issues remain unresolved, such as: (1) which proteins regulate the formation of F-actin; (2) the role(s) of actin polymerization during capacitation; and (3) whether F-actin is a key regulator of the modifications that the sperm membrane undergoes. Our results address these uncertainties.

Studies in somatic cells have suggested that ezrin exists in an inactive, dominant-negative conformation until its Thr₅₆₇ residue is phosphorylated [15, 16]. Using Western blot analysis, we observed that phosphorylation of ezrin on its Thr₅₆₇ residue increases after capacitation, suggesting an increase in the active form of ezrin. We speculate that activated ezrin can then regulate sperm capacitation through its involvement in the ezrin–RhoGDI1–actin–membrane protein network. This hypothesis is supported by the results of our Co-IP experiments in which interaction between ezrin and RhoGDI1 increased after capacitation, suggesting that ezrin has the ability to dissociate RhoGDI1 from RhoA after capacitation. In addition, studies in somatic cells have shown that RhoGDI1 dissociates from Rho through phosphorylation, a modification that we observed in capacitated human sperm. Subsequent Co-IP experiments revealed that RhoGDI1 exhibits decreased binding affinity for RhoA, suggesting that RhoA is released from RhoGDI1 after capacitation. The released RhoA may then promote the formation of F-actin through the Rho-GTPase protein pathway.

We hypothesize that ezrin may be involved in the regulation of human sperm capacitation through the Rho-GTPase protein pathway. In addition, ezrin may be a key player in another pathway that may involve F-actin, ezrin and membrane proteins, and the interaction between these proteins may regulate sperm capacitation. These two pathways seem to be linked through the polymerization of actin, which was shown to be regulated by ezrin and its related proteins in the present

study.

As observed in somatic cells, our study showed that activated ezrin can bind more actin (most likely F-actin) during human sperm capacitation. Moreover, mAb-mediated depletion of ezrin and actin effectively blocked sperm capacitation, indicating that both proteins have important functional roles during this process.

We also examined whether ezrin interacts with membrane proteins during sperm capacitation and, if so, which membrane proteins are implicated in this process. We selected some candidate proteins by reviewing the scientific literature for membrane proteins that were shown to interact with ezrin in somatic cells. Some of these candidate proteins were previously shown to be expressed by human sperm, such as the plasma membrane protein cd44 [30], which was chosen for further study. Our results showed that ezrin binds to cd44 in its native and glycosylated forms. We thus inferred that ezrin and actin might synergistically promote capacitation by interacting with cd44. Although the role of cd44 in sperm has not yet been investigated, studies in other cell types have shown that cd44 is a receptor for hyaluronan [32–34], which is a component of the extracellular matrix. In the oocyte, the extracellular matrix is a key component of the corona radiata [35]. We speculate that cd44 may have a key role in sperm–egg interaction; however, extensive studies are required to confirm this hypothesis. An experimental model is not yet available to study human sperm–oocyte interactions because of the ethical issues involved and the limited availability of samples. Other animal-based models, such as *in vitro* fertilization, are not representative of the role of cd44 in human sperm, making it difficult to assess the role of cd44 in capacitation. However, it is also possible that cd44 may not be the only membrane protein that interacts with ezrin during capacitation.

On the basis of the role of ezrin in membrane remodeling in somatic cells, we postulate that the ezrin–RhoGDI1–actin–membrane protein network has an important role in the modification of membrane characteristics during sperm capacitation, a process that is likely mediated by the relocalization of these membrane proteins (Figure 5). Previous reports have shown that some glycoproteins redistribute during sperm capacitation, which then facilitates the AR reaction and recognition, binding and fusion with the oocyte during fertilization [7, 36, 37]. Thus, this study provides new insights into the remodeling of sperm membrane proteins during capacitation and advances our understanding of capacitation.

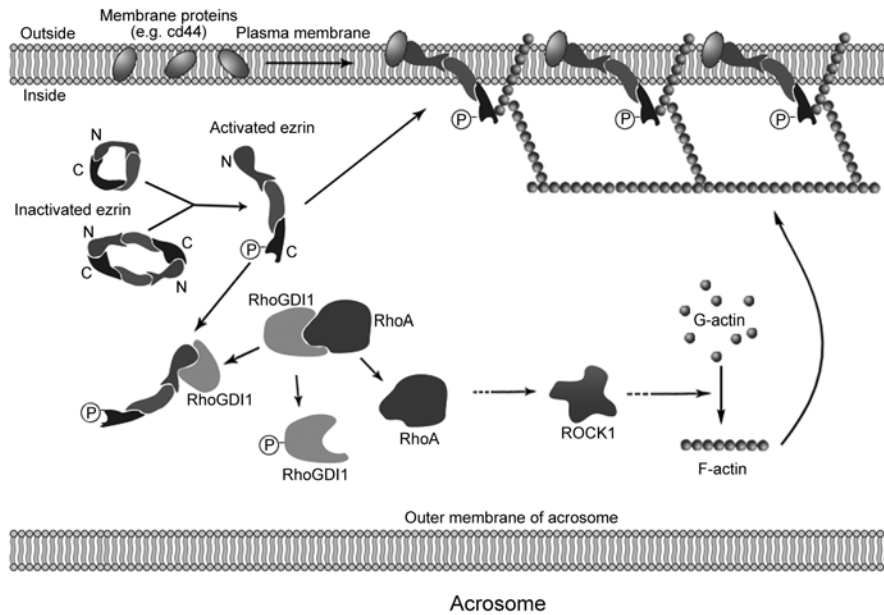


Figure 5. A model of ezrin and its associated protein network in the remodeling of membrane proteins during human sperm capacitation. Before capacitation, ezrin is inactive, with its C-terminal domain associated with the N-terminal domain. During capacitation, ezrin is activated by the phosphorylation of Thr₅₆₇. Activated ezrin then interacts with RhoGDI1, which becomes phosphorylated, causing RhoGDI1 to dissociate from RhoA, leading to actin polymerization. Activated ezrin also interacts with F-actin and membrane proteins (cd44), which can change the location or status of the proteins in the membrane, rendering the sperm capable of undergoing the AR and fertilization.

In summary, our results indicate that, during human sperm capacitation, a network composed of ezrin, RhoGDI1, RhoA, F-actin and membrane proteins influences the fluidity of the sperm membrane to promote capacitation.

Acknowledgment

This work was supported by grants from the 973 program (No. 2006CB504002), the National Natural Science Foundation of China (No. 30630030), the Program for the Scholars of Changjiang and the Innovative Research Team of the University (PCSIRT) (No. IRT0631) and the Jiangsu Youth Technological Innovation Projects Foundation (No. BK2007602).

References

- 1 Baumber J, Meyers SA. Changes in membrane lipid order with capacitation in rhesus macaque (*Macaca mulatta*) spermatozoa. *J Androl* 2006; 27: 578–87.
- 2 Harrison RA, Gadella BM. Bicarbonate-induced membrane processing in sperm capacitation. *Theriogenology* 2005; 63: 342–51.
- 3 Martinez P, Morros A. Membrane lipid dynamics during

- human sperm capacitation. *Front Biosci* 1996; 1: d103–17.
- 4 Companyo M, Iborra A, Villaverde J, Martinez P, Morros A. Membrane fluidity changes in goat sperm induced by cholesterol depletion using beta-cyclodextrin. *Biochim Biophys Acta* 2007; 1768: 2246–55.
- 5 Austin CR. The capacitation of the mammalian sperm. *Nature* 1952; 170: 326.
- 6 Chang MC. Fertilizing capacity of spermatozoa deposited into the fallopian tubes. *Nature* 1951; 168: 697–8.
- 7 Fusi FM, Bronson RA. Sperm surface fibronectin. Expression following capacitation. *J Androl* 1992; 13: 28–35.
- 8 Cohen-Dayag A, Eisenbach M. Potential assays for sperm capacitation in mammals. *Am J Physiol* 1994; 267: C1167–76.
- 9 Shadan S, James PS, Howes EA, Jones R. Cholesterol efflux alters lipid raft stability and distribution during capacitation of boar spermatozoa. *Biol Reprod* 2004; 71: 253–65.
- 10 Gadella BM, Lopes-Cardozo M, van Golde LM, Colenbrander B, Gadella TW Jr. Glycolipid migration from the apical to the equatorial subdomains of the sperm head plasma membrane precedes the acrosome reaction. Evidence for a primary capacitation event in boar spermatozoa. *J Cell Sci* 1995; 108 (Pt 3): 935–46.
- 11 Bretscher A. Purification of an 80,000-dalton protein that is a component of the isolated microvillus cytoskeleton, and its localization in nonmuscle cells. *J Cell Biol* 1983; 97: 425–32.



- 12 Bretscher A, Reczek D, Berryman M. Ezrin: a protein requiring conformational activation to link microfilaments to the plasma membrane in the assembly of cell surface structures. *J Cell Sci* 1997; 110 (Pt 24): 3011–8.
- 13 Tsukita S, Yonemura S. ERM (ezrin/radixin/moesin) family: from cytoskeleton to signal transduction. *Curr Opin Cell Biol* 1997; 9: 70–5.
- 14 Algrain M, Turunen O, Vaheri A, Louvard D, Arpin M. Ezrin contains cytoskeleton and membrane binding domains accounting for its proposed role as a membrane-cytoskeletal linker. *J Cell Biol* 1993; 120: 129–39.
- 15 Zhou R, Zhu L, Kodani A, Hauser P, Yao X, *et al.* Phosphorylation of ezrin on threonine 567 produces a change in secretory phenotype and repolarizes the gastric parietal cell. *J Cell Sci* 2005; 118: 4381–91.
- 16 Gautreau A, Louvard D, Arpin M. Morphogenic effects of ezrin require a phosphorylation-induced transition from oligomers to monomers at the plasma membrane. *J Cell Biol* 2000; 150: 193–203.
- 17 DerMardirossian C, Bokoch GM. GDIs: central regulatory molecules in Rho GTPase activation. *Trends Cell Biol* 2005; 15: 356–63.
- 18 Hall A, Nobes CD. Rho GTPases: molecular switches that control the organization and dynamics of the actin cytoskeleton. *Philos Trans R Soc Lond B Biol Sci* 2000; 355: 965–70.
- 19 Takahashi K, Sasaki T, Mammoto A, Takaishi K, Kameyama T, *et al.* Direct interaction of the Rho GDP dissociation inhibitor with ezrin/radixin/moesin initiates the activation of the Rho small G protein. *J Biol Chem* 1997; 272: 23371–5.
- 20 Brener E, Rubinstein S, Cohen G, Shternall K, Rivlin J, *et al.* Remodeling of the actin cytoskeleton during mammalian sperm capacitation and acrosome reaction. *Biol Reprod* 2003; 68: 837–45.
- 21 Breitbart H, Cohen G, Rubinstein S. Role of actin cytoskeleton in mammalian sperm capacitation and the acrosome reaction. *Reproduction* 2005; 129: 263–8.
- 22 Breitbart H, Rubinstein S, Etkovitz N. Sperm capacitation is regulated by the crosstalk between protein kinase A and C. *Mol Cell Endocrinol.* 2006; 252: 247–9.
- 23 Breitbart H, Rotman T, Rubinstein S, Etkovitz N. Role and regulation of PI3K in sperm capacitation and the acrosome reaction. *Mol Cell Endocrinol.* 2010; 314: 234–8.
- 24 Liu DY, Martic M, Clarke GN, Grkovic I, Garrett C, *et al.* An anti-actin monoclonal antibody inhibits the zona pellucida-induced acrosome reaction and hyperactivated motility of human sperm. *Mol Hum Reprod* 2002; 8: 37–47.
- 25 Liu DY, Clarke GN, Baker HW. Exposure of actin on the surface of the human sperm head during *in vitro* culture relates to sperm morphology, capacitation and zona binding. *Hum Reprod* 2005; 20: 999–1005.
- 26 Liu DY, Martic M, Clarke GN, Dunlop ME, Baker HW. An important role of actin polymerization in the human zona pellucida-induced acrosome reaction. *Mol Hum Reprod* 1999; 5: 941–9.
- 27 Guo XJ, Zhao C, Wang FQ, Zhu YF, Cui YG, *et al.* Investigation of human testis protein heterogeneity using two-dimensional electrophoresis. *J Androl* 2010 (in press).
- 28 World Health Organization. WHO Laboratory manual for the examination of human semen and sperm-cervical mucus interaction. Cambridge: Cambridge University Press.
- 29 Zhu YF, Cui YG, Guo XJ, Wang L, Bi Y, *et al.* Proteomic analysis of effect of hyperthermia on spermatogenesis in adult male mice. *J Proteome Res* 2006; 5: 2217–25.
- 30 Bains R, Adeghe J, Carson RJ. Human sperm cells express CD44. *Fertil Steril* 2002; 78: 307–12.
- 31 Bajorath J. Molecular organization, structural features, and ligand binding characteristics of CD44, a highly variable cell surface glycoprotein with multiple functions. *Proteins* 2000; 39: 103–11.
- 32 Brown KL, Birkenhead D, Lai JC, Li L, Li R, *et al.* Regulation of hyaluronan binding by F-actin and colocalization of CD44 and phosphorylated ezrin/radixin/moesin (ERM) proteins in myeloid cells. *Exp Cell Res* 2005; 303: 400–14.
- 33 Legg JW, Isacke CM. Identification and functional analysis of the ezrin-binding site in the hyaluronan receptor, CD44. *Curr Biol* 1998; 8: 705–8.
- 34 Underhill C. CD44: the hyaluronan receptor. *J Cell Sci* 1992; 103 (Pt 2): 293–8.
- 35 Russell DL, Salustri A. Extracellular matrix of the cumulus-oocyte complex. *Semin Reprod Med* 2006; 24: 217–27.
- 36 Barboni B, Lucidi P, Mattioli M, Berardinelli P. VLA-6 integrin distribution and calcium signalling in capacitated boar sperm. *Mol Reprod Dev* 2001; 59: 322–9.
- 37 Baker SS, Thomas M, Thaler CD. Sperm membrane dynamics assessed by changes in lectin fluorescence before and after capacitation. *J Androl* 2004; 25: 744–51.